ELSEVIER

Contents lists available at ScienceDirect

## **Chemical Physics Letters**

journal homepage: www.elsevier.com/locate/cplett





# Spatial influence of paramagnetic molecules on magnetic tunnel junction-based molecular spintronic devices (MTJMSD)

Marzieh Savadkoohi, Christopher D'Angelo, Andrew Grizzle, Bishnu Dahal, Pawan Tyagi \*

Center for Nanotechnology Research and Education, Mechanical Engineering, University of the District of Columbia, Washington DC-20008, USA

ARTICLE INFO

Keywords: MTJ MSD MTJMSD Molecular spintronics Molecular electronics

#### ABSTRACT

Magnetic Tunnel Junction-Based Molecular Spintronic Devices (MTJMSDs) are potential candidates for inventing highly correlated systems. Understanding MTJMSD's magnetic behavior is essential to designing and fabricating practical devices. This paper investigates the effect of two contributing factors on MTJMSD's magnetic properties via Monte Carlo Simulation. We have systematically studied coupling strengths and nature between magnetic molecules and ferromagnetic electrodes at various temperatures. We have also investigated the effect of length and thickness increase on MTJMSD temporal and spatial evolution of magnetic moment, magnetic correlation, and magnetic susceptibility. Our results showed that thermal energy increase significantly affects molecular devices.

## 1. Introduction

Magnetic tunnel junction-based molecular spintronic devices (MTJMSD) may open new windows toward advancing futuristic electronic and computational instruments and new forms of composite magnetic materials [1]. Utilizing the spin properties of magnetic molecules in an MTJMSD can result in unprecedented magnetic phenomena and produce a variety of novel properties [2]. MTJMSD and its characteristics have been the topic of focus for nearly two decades [1,3,4]. Different techniques such as sandwiching molecules between ferromagnetic (FM) electrodes [5] and using a nanogap junction between FM electrodes [6] have been used to fabricate MSDs. Despite having shortterm success, traditional MSD device fabrication methods suffer from various difficulties (e.g., the negligible opportunity of mass production, molecular damage or distortion during fabrication, atomic-level defects, time-dependent defects, limited FM electrode, and insulator options, etc.) [7]. MTJMSD mainly focus on utilizing paramagnetic molecule as the functional device elements.

It is noteworthy that MTJMSD's focus differs from prior efforts. Molecular spin valves have been extensively examined in past years, where nonmagnetic molecules are usually sandwiched between two ferromagnetic electrodes [5,8]. In these studies, the focus was on molecules' extraordinary long spin coherence length and time [9]. The utilization of nonmagnetic molecules between two ferromagnets limits the scope of molecular spintronics to spin valve-like applications.

Petrove et al. theoretically calculated that interaction between paramagnetic molecules and magnetic electrodes can yield unprecedented > 5 orders of magnitude in resistance change [10,11]. MTJMSD offers a platform to harness paramagnetic molecules. Two representative examples of paramagnetic molecules utilized in MTJMSDs are organometallic molecular clusters (OMC) [12,13] and single-molecule magnets (SMM)[14]. Several OMCs-based MTJMDs and associated intriguing observations are reported elsewhere [1].

MTJMSDs are made of two ferromagnetic electrodes separated by a nanoscale (~2–3 nm) thick insulator (Fig. 1a). In this approach, paramagnetic molecules are covalently attached to the exposed edges of FM electrodes in a cross-junction-shaped MTJ (Fig. 1b) [1]. Connecting molecules to FM electrodes can result in infinite magnetic and transport properties, which can be extremely challenging to test experimentally. Additionally, the theoretical investigation of MTJMSD is complicated due to the possibility of using an extensive range of FM electrodes and complex molecules. Any theoretical analysis of MTJMSD must consider several variables such as molecular coupling to individual FM electrodes, the impact of competing coupling via tunnel barrier and molecules, molecular spin state, etc.

To tackle this problem of understanding MTJMSD and exploring a variety of novel devices and correlated materials, we have used Monte Carlo Simulation (MCS). For the MCS study, we utilized the Heisenberg model of MTJMSD (Fig. 1c), where the properties of molecule and FM electrodes can be parametrically defined in 3D (Fig. 1d) [15].

E-mail address: ptyagi@udc.edu (P. Tyagi).

 $<sup>^{\</sup>ast}$  Corresponding author.

There exists a knowledge gap about the effect of different sizes of MTJMSD on its fundamental properties. Recently, we studied the impact of molecular exchange couplings with the left FM electrode (JmL) and right FM electrode (JmR) on the MTJMSD's magnetic properties [15]. Our previous research showed that the nature and strength of molecular Heisenberg exchange couplings dictated FM electrodes magnetization and defined the entire MTJMSD magnetic behavior for a fixed device size [15]. In another recent study, we have experimentally shown that

current device architecture was inspired by our previous experimental work [17,18] and simulated, as shown in Fig. 1.

We changed the Heisenberg exchange coupling strengths and nature between the paramagnetic molecule and left FM electrode (JmL) and right FM electrode (JmR). To achieve the equilibrium energy state or minimum energy level, we used the continuous Metropolis algorithm and Markov process [1]. System energy was calculated and minimized through the following equation:

$$E = -J_L \left( \sum_{i \in L} \overrightarrow{S}_i \overrightarrow{S}_{i+1} \right) - J_R \left( \sum_{i \in R} \overrightarrow{S}_i \overrightarrow{S}_{i+1} \right) - J_{mL} \left( \sum_{i \in L, i+1 \in mol} \overrightarrow{S}_i \overrightarrow{S}_{i+1} \right) - J_{mR} \left( \sum_{i-1 \in mol, i \in R} \overrightarrow{S}_{i-1} \overrightarrow{S}_i \right)$$
 (1)

MTJMSD's thickness variation results in a  $10^3$  to  $10^6$  times difference in junction conductivity [16,20]. Through magnetic force microscopy (MFM), we have also observed that increasing FM electrode length leads to different magnetic phases along the junction area [17]. This paper reports the impact of device length and thickness variation on MTJMSD's different magnetic properties, such as temporal and spatial evolution of magnetic moment, energy, and magnetic susceptibility. We have also investigated the effect of thermal energy variation on MTJMSD magnetic properties to gain the optimal operating range and find the threshold at which magnetic properties are eradicated due to increasing thermal fluctuations. This study gave us insights into suitable conditions in which various device fabrication can be experimentally realized.

#### 2. Methodology

The MTJMSD device simulated and used in this study was defined with the H  $\times$  W  $\times$  L dimension, where H is the height, W is the width, and L is the length of the device. The molecular plane is along the H side of the device structure and located between an equal number of atomic FM layers (5  $\times$  5). Simulated paramagnetic molecules act as conductive bridges between FM electrodes and make electric charge transport possible in MTJMSD in place of insulators (a.k.a, tunnel barriers). The

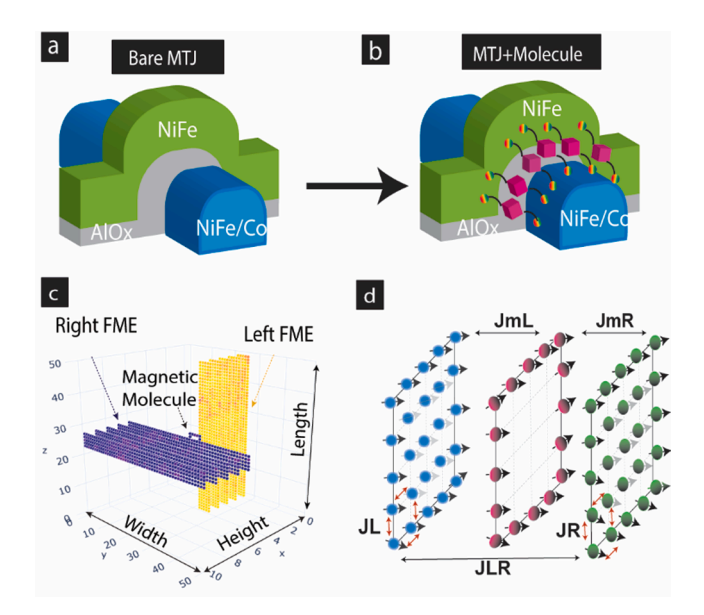


Fig. 1. MTJMSD 3D-architecture (a) before and (b) after magnetic molecules treatment (c) 3D MTJMSD Hisenberg model analogues to MTJMSD in panel (b). (d) Hisenberg model describing inter- and intra-atomic Heisenberg exchange coupling energies between FM electrodes (FMEs) and magnetic molecules.

 $J_L$  and  $J_R$  are inter-atomic exchange couplings in the left and right electrodes. To avoid the over-complexity of our simulation results and too many overlapping effects, we assumed that any leakage or conduction through the tunneling barrier (insulator) is negligible ( $J_{LR}=0$ ). However, we have systematically investigated any chance of intra-FM layers conduction through the insulator elsewhere [18].  $S_{\rm i}$  is the spin vector of atoms in ferromagnetic electrodes and molecules in 3D vectors and has three x, y, and z components.

We performed Heisenberg exchange coupling variation when thermal energy (kT) is varied from 0.1 to 1.1. It is noteworthy that variation in thermal energy is analogous to temperature variation, as thermal energy is obtained by multiplying the Boltzmann constant (k) with temperature. The effect of temperature on MTJMSD occurs via the Metropolis algorithm of MCS used in this study. According to Metropolis, a random spin direction is created in spherical coordinates at randomly selected molecule or ferromagnet site at each new iteration. This new spin state is accepted or rejected based on the difference in MTJMSD energy computed using equation (1). If the difference in MTJMSD ( $\Delta E$ ), i.e., the difference in energy after and before the creation of a new spin direction, is negative new spin direction is accepted. However, when  $\Delta E > 0$ , the newly created random spin direction is accepted or rejected using the Metropolis algorithm [1,19]. Under this algorithm,  $\exp(-\Delta E/kT)$  is compared with a random number between 0 and 1. If  $\exp(-\Delta E/kT)$  is more than the random number, it means at a given thermal energy or temperature new spin state is stable and can be accepted. The system's thermal energy plays a dramatic role in the selection and rejection of new states due to exponential dependency in exp

**Table 1**Different values of thermal energy and device sizes that were used in Monte Carlo Simulation (MCS) to investigate MTJMSD magnetic properties.

MCS study variable	Magnitudes
	$5 \times 50 \times 5$
MTJMSD's length and width	$5 \times 100 \times 5$
(H $\times$ W $\times$ L atomic size)	5  imes 150  imes 5
	5  imes 200  imes 5
	$5 \times 50 \times 5$
MTJMSD's thickness	10  imes 50  imes 5
(H $\times$ W $\times$ L atomic size)	$15\times 50\times 5$
	$20\times 50\times 5$
	$25\times50\times5$
	0.05
Thermal Energy(kT)	0.1
	0.3
	0.7
	0.9
	1.1

 $(-\Delta E/kT)$ . It is noteworthy that many new states are rejected at very low thermal energy, and systems tend to form long-range ordering. However, it is challenging to stabilize a single phase at higher thermal energy, and multiple comparable energy configurations are possible. Multiple stable spin directions at higher thermal energy represent noise in the system. This thermal energy is representative of dominant thermal fluctuations in ferromagnets. However, since we did not vary characteristics of lattice parameters or itinerant electrons exclusively, we cannot associate thermal fluctuations to a specific physical source.

The device dimension was then changed in length and thickness, as shown in Table 1. For different device sizes, we conducted various simulation counts ( $\sim\!200$  M to 2B). We studied the spatial and temporal evolution of MTJMSD's magnetic moment (M) as a function of JmL and JmR. We also have varied thermal energy values between -1 to 1 (Table 1) with the step of 0.1 for our fixed standard device size (5  $\times$  50  $\times$  5). The goal was to attain the optimal range of thermal energy in which MTJMSD can operate efficiently and is not negatively affected by exceeded thermal energy effect. To investigate the impact of thermal energy and device size on MTJMSD's magnetic properties, we conducted a systematic study of MTJMSD's temporal and spatial evolution of magnetic moment (M), and the magnetic correlation between FM electrodes via molecules, and magnetic susceptibility.

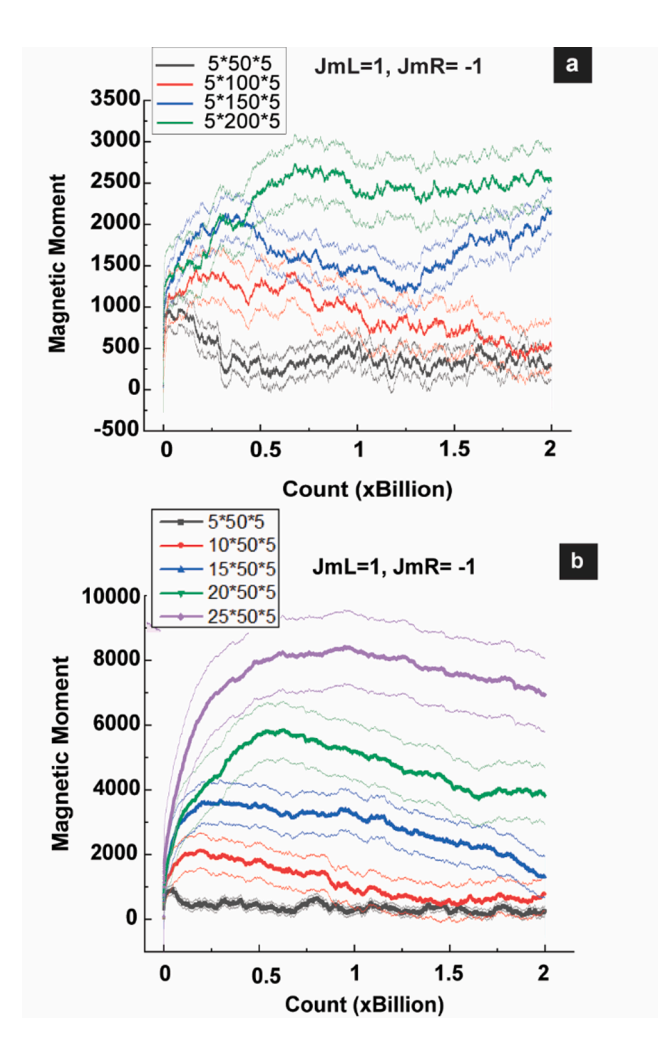


Fig. 2. Average  $\pm$  standard error of Temporal evolution of MTJMSD magnetic moment when magnetic molecules made ferromagnetic coupling with the left electrode ( $J_{mL}=1$ ) and antiferromagnetic coupling with the right electrode ( $J_{mR}=$ -1) for MTJMSD (a) increased length (b) increased thickness.

#### 3. Results and discussion

To understand the length and thickness effect mechanism, we conducted an MCS study by varying the FM electrode length and thickness, while 16 molecular analogs were used in all studies. If two electrodes aligned perfectly antiparallel due to strong antiferromagnetic coupling, an MTJMSD will show near-16 magnetic moment. On the other hand, if multiple magnetic phases evolve within FM electrodes and around the junction due to increased length or thickness, the overall magnetic moment will vary between the lowest and highest magnetic moment. Fig. 2 represents the average of three repetitions and standard deviations of the temporal evolution of MTJMSD magnetic moment for different device sizes. To investigate the effect of device size on MTJMSD evolution to the equilibrium state, we ran an MCS simulation in the 200 million < iterations < 2 billion range. To compare the MTJMSD evolution at the same time scale, we compared data for 2 billion iterations. To investigate the strong molecule-induced coupling effect, we fixed ferromagnetic coupling between molecules with one FM electrode ( $J_{mL}$ = 1) and antiferromagnetic coupling with another FM electrode ( $J_{mR}$  = -1). This selection of  $J_{mL}$  and  $J_{mR}$  was inspired by our previous experimental work providing evidence of molecule induced strong antiferromagnetic coupling [1].

Magnetic moment vs. iteration count data shows that MTJMSD with 5 atom width, 5 atom thickness, and 50 atom length settled  $\sim 200$  magnetic moments (Fig. 2a). As discussed elsewhere in this paper, the two electrodes' magnetic moment was stabilizing in an antiparallel state throughout the length and thickness of the device. However, with the increasing length, it became increasingly challenging to stabilize in a low magnetic moment state (Fig. 2a). For the MTJMSD with 200 atoms, long FM electrode MTJMSD stayed in  $\sim$  a 2500 magnetic moment state.

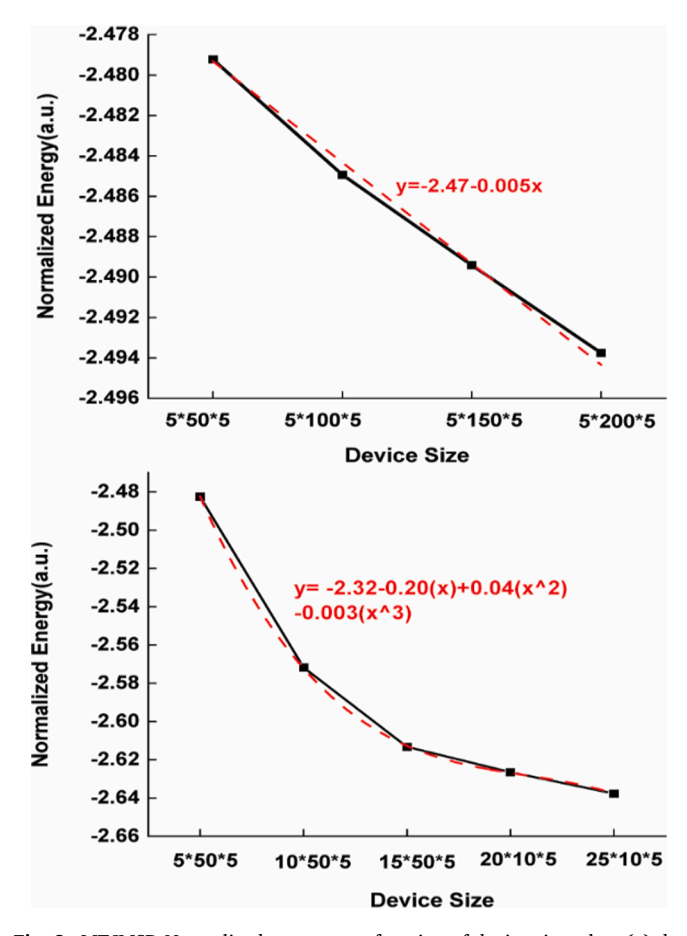
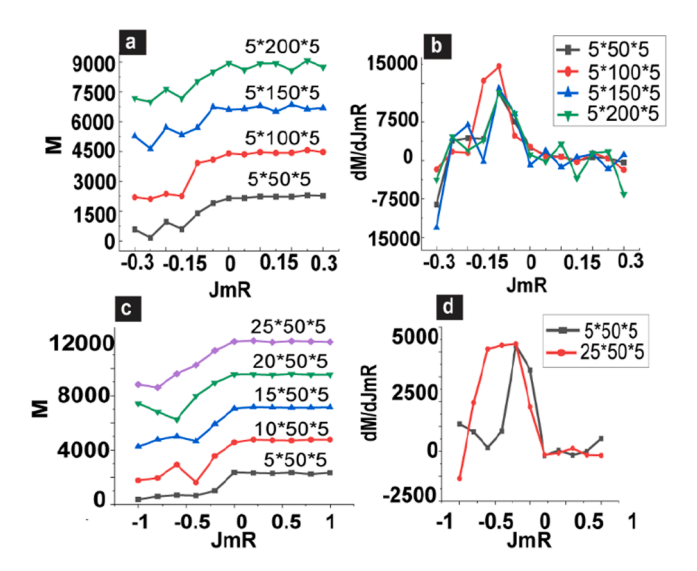


Fig. 3. MTJMSD Normalized energy as a function of device size when (a) device length increased (b) device thickness increased.

A similar trend was observed when the thickness of the FM electrode increased from 5 to 25 (Fig. 2b). However, magnetic moment fluctuations were more pronounced when the length was varied (Fig. 2a-b). Increasing length appears to develop a variety of magnetic phases away from the junction area and will be investigated further elsewhere in this paper. This means that 16 molecules used in the MTJMSD's Heisenberg model were capable of enforcing antiferromagnetic coupling impact for smaller FM electrode thickness and length only. Our recent publication investigated the effect of size increase on the spatial evolution of MTJMSD's magnetic moment at the atomic level [20]. Our results showed that increasing device dimension results in weaker induced molecular impact and many magnetic phases along the FM electrodes. This result agrees with the increased temporal evolution of magnetic moment to 2 billion counts for larger device sizes discussed in this paper.

We also investigated the energy of MTJMSD and found that with increasing MTJMSD's length and thickness, energy decreases (Fig. 3). The normalized lowest energy magnitude that each device gained through the Metropolis algorithm and Markov process after 2B simulation counts is shown in figue.3. Fig. 3(a-b) shows that the equilibrium energy state decreases as device size increases in a robust molecule-FM electrode coupling regimen ( $J_{mL} = 1$ ,  $J_{mR} = -1$ ). The inverse relationship between MTJMSD size and energy state can be interpreted as having various magnetic behaviors. For instance, increased size devices can be considered suitable testbeds to create stable metamaterials, while smaller devices are more switchable in the presence of an external magnetic field. The required energy can be calculated for different device lengths and thicknesses to gain a stable equilibrium state. As the results implied, the energy trendline is linear when device length increases (Fig. 3a). Therefore, the equilibrium energy decreases proportionally between various device sizes for more extended FM electrodes. However, increasing thickness shows a polynomial fitting (Fig. 3b). Therefore, a higher rate of energy is required to make the transition happen from high to low magnetization in molecule-FM electrodes' antiferromagnetic coupling regimen.

To estimate the critical molecular coupling required to transition MTJMSD from a high to low magnetization state, we varied JmL and JmR for different FM electrode lengths and thicknesses. Since most of the  $J_{mL}$  and  $J_{mR}$  effects are symmetrical, we strategize to fix  $J_{mL}$  to 1 and vary  $J_{mR}$  from -1 to 1. We observed a major change in the -0.3 to 0.3



**Fig. 4.** Two-dimensional illustration of (a) MTJMSD's magnetic moment (M) as a function of JmR for JmL=1 when device length increased (b) First derivative of MTJMSD's magnetic moment with respect to JmR, when device length increased (c) MTJMSD's magnetic moment (M) as a function of JmR for JmL=1 when device thickness increased (d) First derivative of MTJMSD's magnetic moment with respect to JmR, when device thickness increased.

range (Fig. 4a). To distinguish the transition point, we took the first derivative of magnetic moment with respect to  $J_{mR}$  for MTJMSD with FM electrodes of different lengths (Fig. 4b). The derivative plot clearly shows that irrespective of FM electrode length, critical molecular coupling strength was  $\sim$  -0.15 (Fig. 4b). These results suggest that FM electrode length does not influence the transition in the molecular junction area.

In the same vein, we also studied the effect of  $J_{mL}$  and  $J_{mR}$  on various FM electrode thicknesses (Fig. 4c). Increasing FM electrode thickness expanded the  $J_{mR}$  range over which MTJMSD high to low magnetic moment transition occurred. To distinguish the transition range, we plotted the first derivative of MTJMSD magnetization with respect to  $J_{mR}$  (Fig. 4d). Transition for the 5 atomic unit thick FM electrode was sharp and confined around  $\sim 0.15$ . However, the transition for the 25atom thick FM electrode-based MTJMSD spread from 0 to  $\sim$  0.75. This result also provides valuable insight for the I-V study we did in our previous work showing ~ 1000 times more current suppression from thinner FM electrode-based MTJMSD. Thicker FM electrodes yield significantly unstable and  $\sim 10$  nA range current suppression as opposed to pA level current suppression [17]. It is noteworthy that pA level current suppression is expected when two FM electrodes are completely antiparallel to each other. Two fully antiparallel magnetic electrodes cancel the magnetic moment of each other and produce near zero MTJMSD magnetic moment. As shown in the comparative study in Fig. 4c-d, 5 atom thick FM electrode can become completely antiparallel to each other with the help of ~ 0.2 magnitude of molecule induced exchange coupling. However, increasing FM thickness to 25 atoms do not become parallel to each. Increasing FM electrode thickness to 25 expanded the  $J_{mR}$  range from 0.2 to 0.75 over which MTJMSD high to partial low magnetic moment transition occurred. For the observation of pA level current magnetic moment is expected to settle close to zero. However, with increasing thickness magnetic moment always remain significant suggesting that two FM electrodes are not canceling the magnetic moment of each other and hence some intermediate MTJMSD state (e.g. ~ 10 nA current state) is expected. Further discussion about the MCS results and current suppression is also discussed elsewhere

MTJMSD discussed in this paper are expected to respond to the magnetic field. To evaluate how different zones of the FM electrode will respond to an external magnetic field, we calculated spatial magnetic susceptibility. For magnetic susceptibility calculation, FM electrode atoms along the width were included. Magnetic susceptibility for the MTJMSD with 5x50x5 dimension is shown in Fig. 5a. Data in Fig. 5a suggest that molecules are more susceptible to the magnetic field as compared to the FM electrode. Higher molecule susceptibility was observed for 200 atom long FM electrodes (Fig. 5b) and 25 atom thick FM electrodes (Fig. 5c). Interestingly, magnetic susceptibility was 1–1.2 in the molecular region, while FM electrodes show the considerably lower non-uniform distribution of magnetic susceptibility values of |-0.2| to |-0.4| spread all over the area. This observation tells us that molecules can selectively respond to the external magnetic field, and we can expect a switching phenomenon if the molecule can switch states.

## A. Thermal energy effect on MTJMSD's magnetic properties

Thermal energy (kT) was varied between 0.05 and 1.1 of the Curie temperature with step 0.2. We kept the device dimension constant at this time and used our standard MTJMSD size of  $5\times50\times5$ . The magnetic moment was studied as a function JmR, kT and JmL was kept constant (JmL = -1). Fig. 6(a) shows the contour plot of M variation regarding kT and JmR when JmL = -1. Total device magnetization can settle between 0 and 2500 magnitude due to MTJMSD size. As seen in Fig. 6 (a), induced parallel coupling between FM electrodes (JmL = -1 and  $-1 \leq$  JmR  $\leq$  0) resulted in a magnetic moment increase up to 2250 when 0.05  $\leq$  kT < 0.3. Similarly, a strong annihilated coupling (M  $\approx$  140) between left and right electrodes is observed for the same range of kT values

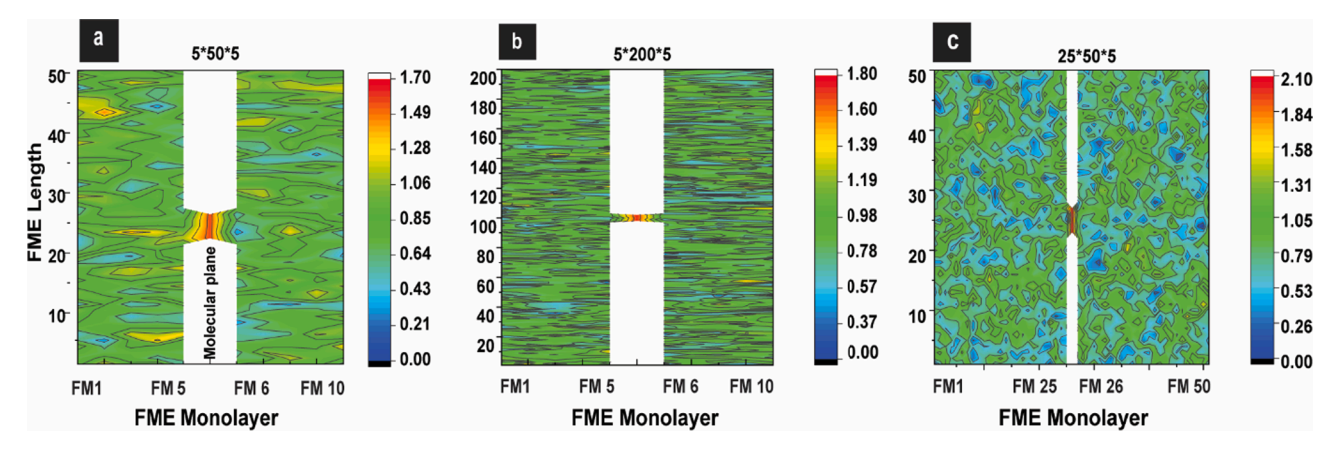
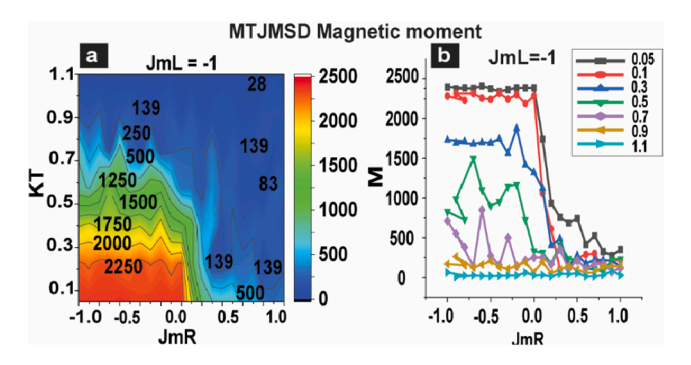


Fig. 5. Magnetic Susceptibility contour plots of MTJMSD for all layers of left and right FM electrodes and the magnetic molecule when  $J_{mL} = 1$ ,  $J_{mR} = -1$ , for device with FM electrodes of (a) 50 atom length and 5 atom thickness, (b) 200 atom length and 5 atom thickness (c) 50 atom length and 25 atom thickness. Width of FM electrode was 5 atom.



**Fig. 6.** (a) Contour plot of MTJMSD's magnetic moment, as a function of KT and FMEs-molecule Heisenberg exchange coupling JmR for JmL = -1 (b) Two-dimensional illustration of MTJMSD's magnetic moment as a function of JmR at different KTs for JmL = -1.

wherever JmL = -1 and  $0 \le JmR \le 1$ . For kT values between  $0.3 \le kT \le 1$ 0.7, we see that magnetic moment is affected by thermal energy fluctuations. An increase in thermal energy does not allow molecules to induce ferromagnetic and antiferromagnetic coupling between FM electrodes efficiently. Thus, the maximum magnetic moment that MTJMSD can gain in this temperature range is about that of an individual FM electrode (~1750-1250). Further increase in temperature  $(0.7 \le kT \le 1.1)$  kills the effect of molecular-induced coupling completely. Total device magnetization is consistently<500 magnitude at this high-temperature range which reflects the opposite spin orientation of atoms in both ferromagnetic and antiferromagnetic induced coupling states. Fig. 6(b) represents the effect of temperature variation on the magnetic moment in 2D. As a result, at kT values ≤ 0.3 of the Curie temperature, 16 molecules can induce ferromagnetic solid and antiferromagnetic coupling between two electrodes. However, starting kT = 0.5 we see that thermal fluctuation is the dominant factor and does not let the system reach the equilibrium energy despite having 2B simulation counts. At kT values of 0.9 and 1.1 of the Curie temperature, the system is completely agitated, and no molecular-induced coupling effect is observed. According to our MCS results, a stable antiferromagnetic and ferromagnetic coupling via magnetic molecules is optimally attainable at room temperature and even slightly above room temperature. However, higher kT values (≥0.3 of the Curie temperature) can critically impact molecular-induced coupling.

## 4. Conclusion

Our simulation results suggest that the temporal evolution of

magnetic moment is extremely longer in larger MTJMSD devices. Also, increasing device length by more than a specific value compromises the molecular induce coupling effect and makes striped-shaped spin orientation within FM electrodes. Interestingly, the transition from low to high magnetization occurred at 15% of the Curie temperature consistently when the device length increased. However, increasing FM-electrodes' thickness made a noticeable change in the required energy to make transitions possible. The critical point in the latter case shifted to around 0.6 of the Curie temperatures for the thickest device case. We also varied the thermal energy (kT) range between 0.05 and 1.1 of the Curie temperatures and studied its impact on MTJMSD's magnetic properties. Our MCS study showed that lower temperatures ( $\sim$ 0.05–0.1) produce stability and allow the molecular-induced coupling to dictate MTJMSD's magnetic and transport properties. This resulted in MTJMSD having zero to the maximum total magnetic moment. However, a further increase in temperature (kT > 0.3) annihilated the effect of molecularinduced magnetic coupling between electrodes and created dominant noises. Thermal energy-induced fluctuations resulted in very low magnetic moments all over the MTJMSD device. This comprehensive study may provide insight into optimal conditions needed to experimentally realize and test MTJMSD devices.

## **Declaration of Competing Interest**

The authors declare that they have no known competing financial interests or personal relationships that could have appeared to influence the work reported in this paper.

## Acknowledgment

We gratefully acknowledge the National Science Foundation-CREST Award (Contract # HRD- 1914751) and the Department of Energy/National Nuclear Security Agency (DE-FOA-0003945).

## References

- P. Tyagi, C. Baker, C. D'Angelo, Paramagnetic Molecule Induced Strong Antiferromagnetic Exchange Coupling on a Magnetic Tunnel Junction Based Molecular Spintronics Device, Nanotechnology 26 (30) (2015) 305602.
- [2] H.B. Heersche, Z. de Groot, J.A. Folk, H.S.J. van der Zant, C. Romeike, M. R. Wegewijs, L. Zobbi, D. Barreca, E. Tondello, A. Cornia, Electron transport through single Mn-12 molecular magnets, Phys. Rev. Lett. 96, (20) (2006), 206801.
- [3] P. Tyagi, 'PhD Thesis: Fabrication and Characterization of Molecular Spintronics Devices, University of Kentucky (<a href="http://archive.uky.edu/handle/10225/878">http://archive.uky.edu/handle/10225/878</a>), 2008
- [4] P. Tyagi, 'Trenched Bottom Electrode and Liftoff based Molecular Devices. US Patent Application No. 16/102,732.' 2020.
- [5] J.R. Petta, S.K. Slater, D.C. Ralph, Spin-dependent transport in molecular tunnel junctions, Phys. Rev. Lett. 93, (13) (2004), 136601.

- [6] A.N. Pasupathy, R.C. Bialczak, J. Martinek, J.E. Grose, L.A.K. Donev, P.L. McEuen, D.C. Ralph, The Kondo effect in the presence of ferromagnetism, Science 306 (5693) (2004) 86–89.
- [7] P. Tyagi, Multilayer Edge Molecular Electronics Devices: A Review, J. Mater. Chem. 21 (13) (2011) 4733–4742.
- [8] A.R. Rocha, V.M. Garcia-Suarez, S.W. Bailey, C.J. Lambert, J. Ferrer, S. Sanvito, Towards molecular spintronics, Nat. Mater. 4 (4) (2005) 335–339.
- [9] M. Ouyang, D.D. Awschalom, Coherent spin transfer between molecularly bridged quantum dots, Science 301 (5636) (2003) 1074–1078.
- [10] E.G. Petrov, I.S. Tolokh, V. May, Magnetic field control of an electron tunnel current through a molecular wire, J. Chem. Phys. 108 (11) (1998) 4386–4396.
- [11] E.G. Petrov, I.S. Tolokh, A.A. Demidenko, V.V. Gorbach, Electron-Transfer Properties of Quantum Molecular Wires, Chem. Phys. 193 (3) (1995) 237–253.
- [12] D.F. Li, S. Parkin, G.B. Wang, G.T. Yee, R. Clerac, W. Wernsdorfer, S.M. Holmes, An S=6 cyanide-bridged octanuclear (Fe4Ni4II)-Ni-III complex that exhibits slow relaxation of the magnetization, J. Am. Chem. Soc. 128 (13) (2006) 4214–4215.
- [13] D. Li, S. Parkin, R. Clérac, S.M. Holmes, Ancillary Ligand Functionalization of Cyanide-Bridged S = 6 FeIII4NiII4 Complexes for Molecule-Based Electronics, Inorg. Chem. 45 (19) (2006) 7569–7571.

- [14] C. Rojas-Dotti, J. Martínez-Lillo, Thioester-functionalised and oxime-based hexametallic manganese (III) single-molecule magnets, RSC Adv. 7 (77) (2017) 48841–48847.
- [15] M. Savadkoohi, B.R. Dahal, A. Grizzle, C. D'Angelo, P. Tyagi, Interaction between magnetic molecules and two ferromagnetic electrodes of a magnetic tunnel junction (MTJ), J. Magn. Magn. Mater. 529 (2021) 167902.
- [16] P. Tyagi, E. Friebe, Large Resistance Change on Magnetic Tunnel Junction based Molecular Spintronics Devices, J. Mag. Mag. Mat. 453 (2018) 186–192.
- [17] P. Tyagi, C. Riso, E. Friebe, Magnetic Tunnel Junction Based Molecular Spintronics Devices Exhibiting Current Suppression At Room Temperature, Org. Electron. 64 (2019) 188–194.
- [18] H. Brown, A. Grizzle, C. D'Angelo, B.R. Dahal, P. Tyagi, Impact of direct exchange coupling via the insulator on the magnetic tunnel junction based molecular spintronics devices with competing molecule induced inter-electrode coupling, AIP Adv. 11 (1) (2021) 015228.
- [19] M.E. Newman, G.T. Barkema, Monte Carlo Methods in Statistical Physics, Clarendon Press, 1999, 1999.
- [20] M. Savadkoohi, C. D'Angelo, A. Grizzle, B. Dahal, P. Tyagi, Impact of ferromagnetic electrode length and thickness on Magnetic Tunnel Junction-Based Molecular Spintronic Devices (MTJMSD), Org. Electron. 102 (2022) 106429.